EUROPEAN ORGANISATION FOR NUCLEAR RESEARCH

CERN/SPSLC 94-25
SPSLC P282
October 10, 1994

Proposal

Neutron halo and antiproton - nucleus potential from antiprotonic X-rays

J. Jastrzębski*, M. Kisieliński, P. Lubiński, L. Pieńkowski, A. Trzcińska
Heavy Ion Laboratory, Warsaw University, PL-02-097 Warsaw, Poland

J. Skalski, R. Smolańczuk, S. Wycech
Soltan Institute for Nuclear Studies, PL-00-681, Warsaw, Poland

K. Gulda, W. Kurcewicz*
Institute of Experimental Physics, Warsaw University, PL-00-681, Warsaw, Poland

T. von Egidy, F.J. Hartmann, S. Schmid, W. Schmid
Physik Department, Technische Universität München, D-85747 Garching, Germany

ABSTRACT

It is proposed to investigate the characteristics of antiprotonic X-rays in a number of heavy nuclei. The objective of this study is a combined analysis of observables depending on the nuclear periphery and the antiproton-nucleus optical potential. These observables would be gathered during the realisation of the proposed program (X-rays level shifts and widths) and will also come from the previous neutron halo investigation performed within the PS203 experiment. The present Proposal demonstrates that such an analysis will substantially improve our knowledge of the nuclear periphery in heavy nuclei and, at the same time, will substantially delimitate the parameters defining the antiproton-nucleus optical potential. In 1995 we request 3 weeks of the beam time for this experiment (about 10^5 $\bar{p}$/s, 200 MeV/c).

Contents

A. INTRODUCTION

Recently, within the PS203 experiment, we have found a new, simple method to study the nuclear periphery composition [JAS93] using the annihilation of stopped antiprotons. This method, described in more detail below, was subsequently applied to a number of nuclei. The presently available results clearly indicate that the periphery of some heavy nuclei is rich in neutrons; the name "neutron halo" is probably the best term for the observed phenomenon.

The neutron and proton densities [LUB94] calculated using a simple Asymptotic Density Model or a more complex Hartree-Fock approach are in qualitative agreement with the experimental results. The calculations clearly indicate the increase of the neutron to proton density ratio at large nuclear distances for nuclei in which a neutron halo was observed. However, at the present stage of the theory the quantitative, parameter free, description of the experimental data is difficult, if not impossible. This is due to the poor knowledge of the antiproton-nucleus optical potential (discussed in more detail below), especially in the case of heavy nuclei.

To achieve further progress in the understanding of the nuclear periphery as well as of the antiproton-nucleus optical potential we propose here a so-called Combined Analysis approach. This approach, strongly advocated e.g. in [BAT89] "could remove some of the model dependence and improve one's understanding of the model involved and thus apply additional information on nuclear densities". It would consist, roughly speaking, in an increase of the number of observables depending on the nuclear density and antiproton-nucleus potential.

Our new method of the nuclear periphery study furnishes two observables which can be compared with theory. We propose to add three more (and in some cases up to six) of them, determining widths, shifts and line splittings in antiprotonic atoms of the same nuclei in which the neutron halo factor was previously determined.

It is worth noting here that the presently available data on antiprotonic X-rays in heavy nuclei (above oxygen) are very limited. The pre-LEAR data (reviewed in [BAT81b]) suffer from low statistics and/or limited accuracy. A few measurements with LEAR beam [POT85, KAN86, DAN87, KRE88a, KRE88b, WYC93] were analysed using the same neutron and proton peripheral density. There are no experiments on level shifts and widths for the same nuclei for which we have determined the ratio of neutron to proton densities.

Section B of this Proposal gives in more detail the presently available information on the neutron halo in heavy nuclei. The various antiproton-nucleus optical potentials are also reviewed there. The proposed experiment is presented and analysed in Section C. Finally, Summary and Conclusions are given in Section D.

B. PHYSICS CASE

1. Neutron halo in heavy nuclei

1.1. Introduction

The shape and composition of the nuclear surface has attracted interest almost from the beginning of nuclear physics [BAT89]. The stimulating paper of Johnson and Teller [JOH54] with the suggestion that the nuclear atmosphere is rich in neutrons even for nuclei close to the beta stability line appeared already in 1954 and generated a long going discussion on this subject. Although eventually the main assumption of this work, namely the equality of the proton potential to the algebraic sum of the neutron and Coulomb potentials, was shown to be incorrect, the interest in nuclear surface composition has not ended by this finding. However, at the end of the sixties it became clear that this composition is the effect of a subtle balance between Coulomb and asymmetry effects [JAC74] and can only be guessed from calculations involving a rather high degree of sophistication [NEG70].

Recently, the "neutron skin", often understood as the difference between the rms radii of neutrons and protons, $\Delta R_{np}^{rms} = R_n^{rms} - R_p^{rms}$, was found to be as large as 0.9 fm in some neutron rich light nuclei [HAN 87, HAN 91, TAN92]. This corresponds to about 40 % relative difference in these radii. The presently available theoretical and experimental information for heavy nuclei close to the beta stability line indicates, in spite of their large neutron excess, much smaller values for the neutron skin in these nuclei. For instance, the Hartree-Fock calculations [NEG70] of the charge and neutron rms radii in ^{208}Pb give a neutron skin of a thickness of 0.23 fm or the relative difference between neutron and proton radii, $\Delta R_{np}/R_0 = 4$ % (where $R_0 = 1/2\,(R_n+R_p)$). The experimental evidence confirms the theoretically calculated values, at least in some cases. Recently, the analysis of the electric giant dipole resonance cross section for α-particle induced excitation [KRA91] gives e.g. the $\Delta R_{np}/R_0$ ratio in ^{48}Ca equal to $(4.1^{+2.1}_{-2.5})$ % and in ^{208}Pb equal to (3.0±1.3) %.

Although a rather small value for the neutron skin in heavy nuclei seems to be now well established, this is by no means the whole story of the nuclear surface composition. Already in 1971, via the study of sub-Coulomb (p,d) and (d,t) reactions it was shown [KÖR71] that at large nuclear distances (significantly above the rms radius) the neutron density of ^{208}Pb exceeds the proton density by orders of magnitude. The study of the interaction of stopped negative kaons [DAV67, BUR67] and antiprotons [BUG73] with heavy nuclei, clearly a peripheral process, also indicated a high neutron to proton density ratio at large, although not well defined, nuclear distances.

The situation when there is no substantial difference between the first moment (rms radius) of the neutron and proton distribution, but a strong enhancement of the neutron density

appears at distances where the matter density is very low, can be called a "neutron halo". Indeed, such a name was already used more than twenty years ago [NOL69] to describe the predominance of neutrons at the nuclear surface. This terminology is adopted throughout this Proposal.

1.2. Probing the nuclear periphery with antiprotons and kaons

Energetic antiprotons are slowed down in matter by interacting with atomic electrons. When their kinetic energy drops well below one keV they are captured in high-n orbits, forming an "exotic atom". As lower orbits in this antiprotonic atom are empty, the antiproton cascades toward the nuclear surface, first emitting Auger-electrons and later predominantly X-rays. The antiprotonic cascade terminates far above the lowest Bohr orbit, when the antiproton encounters a nucleon on the nuclear surface and annihilates. For nuclei like ^{208}Pb, the lowest accessible antiproton orbits have the principal quantum number $n = 9$ or 10 which corresponds to the orbit radius of ≈ 30 fm, much larger than the rms radius of the nuclear matter distribution in this nucleus. The maximum of the annihilation probability is situated at a distance equal to about twice the rms radius. The above scenario, with some changes in orbit number and radius, is also valid for negative kaons. Therefore, if an isospin signature of the annihilation could be found, negative hadrons could be used to probe the composition of the nuclear periphery.

This idea is more than a quarter of a century old. Promoted by Jones [JON58] and Wilkinson [WIL59] it was first experimentally realised by Davis et al. [DAV67] who studied the K^- meson interaction with nuclei in nuclear emulsions. The differences in the characteristics of hyperonic and mesonic reaction products after kaon absorption on a proton or on a neutron were used as the isospin signature of the absorption (due to charge conservation the $\Sigma^+\pi^-$ and $\Sigma^-\pi^+$ reaction products signal the absorption on a proton, whereas the observation of $\Sigma^-\pi^0$ channel implies K^- absorption by a neutron). The emulsion experiment allowed to classify the observed events in two groups: absorptions on light nuclei, characterised by a significant recoil of the nucleus, and absorptions on heavy nuclei (Ag, Br), accompanied by Auger electron tracks. It was found [BUR67, BUR72] that the absorption of K^- on a neutron is about 5 times more probable in heavy than in light nuclei. Knowing, that the K^- absorption takes place in nuclear periphery and assuming a similar neutron and proton distribution in light nuclei this result would indicate an observation of a neutron halo in heavy nuclei [BUR67]. However, it was later shown [WYC71, ASL70, BAT89] that the reported experimental data may be also explained without the assumption of a substantial difference between neutron and proton density at the nuclear periphery.

Besides kaons, antiprotons were also used for the search of a neutron halo in heavy nuclei. In 1973 Bugg et al. [BUG73] presented the results of their experiment in which the Brookhaven National Laboratory 30-inch hydrogen bubble chamber was exposed to a beam of slow antiprotons. In this chamber the mesonic prongs from carbon, titanium, tantalum and lead

targets were investigated. The physics of the experiment was derived from the fact that $\bar{p}p$ and $\bar{p}n$ annihilations produce events with a net charge of 0 and -1, respectively, and from the assumption that the nuclear capture and annihilation processes occur in the nuclear periphery. The net result was expressed as "halo factor", f (in which corrections for the differences in the $\bar{p}n$ and $\bar{p}p$ interaction potentials and target N/Z ratios were taken into account). This factor showed a tendency to increase as a function of the target mass. For the Pb target it was equal to 2.3 ± 0.5 to be compared with the value 1.0 for carbon. The authors of Reference [BUG73] claimed this result to be the evidence of the neutron halo in heavy nuclei.

However, the necessity to apply numerous corrections to the experimental data has obscured the transparency of the conclusions. Moreover, their subsequent criticism [GER74] based on a possible charge exchange process not taken into account in the corrections applied made the question legitimate of whether the neutron halo was really observed in Bugg's experiment.

Recently a new method for the detection of the neutron halo in heavy nuclei using annihilation of stopped antiprotons [JAS93] was found. The method uses the identification of nuclear rather than mesonic products of the antiproton-nucleus interaction.

The new method relies on the simple observation that for antiproton annihilations at distant orbits there is a large probability, P_{miss}, that all pions created during the annihilation miss the target nucleus. As a result, a cold nucleus with mass number $(A_t - 1)$ is produced (here A_t = target mass number).The ratio of nuclei produced with one neutron less than N_t to nuclei with one proton less than Z_t is a function of the neutron to proton density at distances r, where the product of $P_{miss}(r)$ and the antiproton annihilation probability W(r) is sizeable. If $(N_t - 1)$ and $(Z_t - 1)$ products are radioactive their production rate can be easily determined using gamma-ray spectroscopy methods. This enables one to extract a "halo factor"

$$f_{halo} = \frac{N(\bar{p}n)\mathrm{Im}(a_p)Z_t}{N(\bar{p}p)\mathrm{Im}(a_n)N_t}$$

where a_p and a_n are $\bar{p}p$ and $\bar{p}n$ scattering lengths, respectively. The ratio $\mathrm{Im}(a_p)/\mathrm{Im}(a_n)$ is taken from [BUG73]. (It is the ratio of the antiproton annihilation probability with a proton to that with a neutron).

The two observables of interest are the absolute yields of the two radioactive products with mass number $(A_t - 1)$ (number of nuclei produced by 1000 $\bar{p}$) and their ratio, eventually transformed into the halo factor. When the halo factor is related to the neutron to proton density ratio, the absolute yield of $(A_t - 1)$ nuclei is a signature of the annihilation site: for the same W(r) a larger yield of $(A_t - 1)$ nuclei indicates more distant annihilations.

The calculated neutron and proton densities, the antiproton absorption probabilities and the missing probability are shown in Fig. 1 for the target nucleus ^{232}Th. From this figure it can be estimated that the new method probes the nuclear density at distances around about twice the root mean square radius of this nucleus.

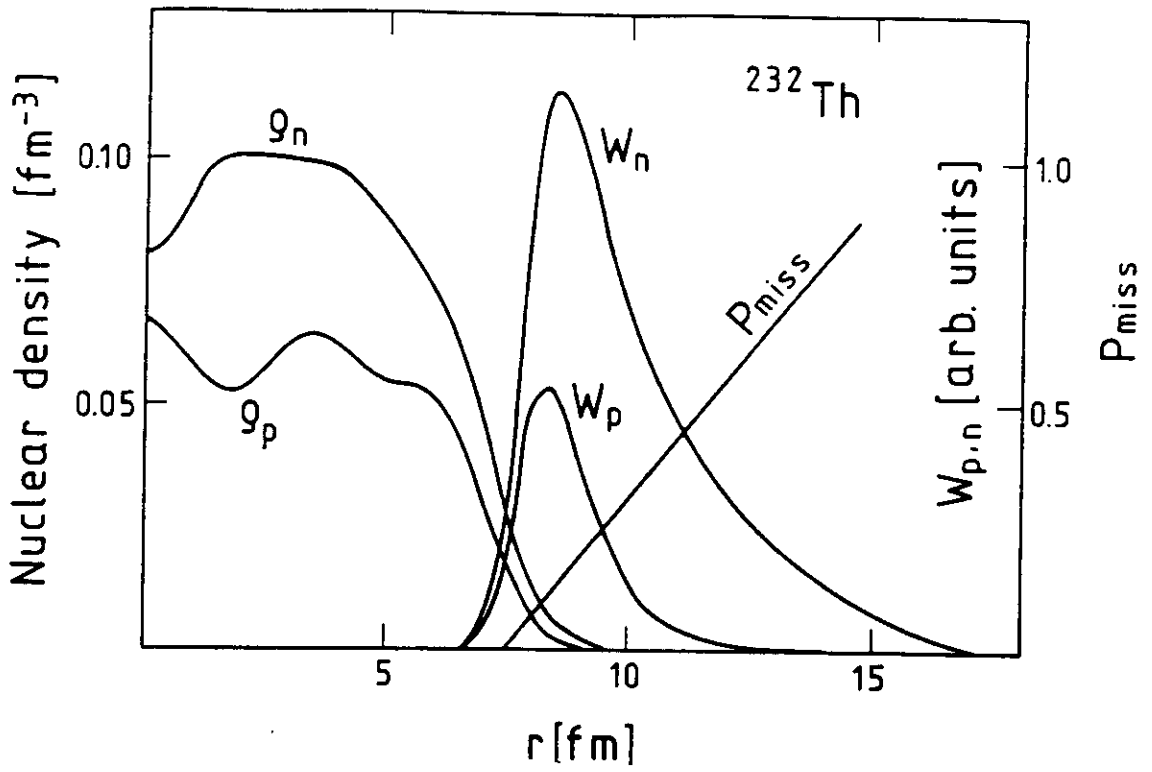

Fig. 1. *Neutron and proton densities, ρ_n and ρ_p, the antiproton absorption probability on neutrons, W_n, and on protons, W_p, and the "missing probability", P_{miss}, for ^{232}Th nucleus. This figure is reproduced from [JAS 93].*

1.3. The most recent news

After the publication of the principle of the new method and the first results for ^{232}Th [JAS93] a number of targets were investigated using antiprotons from the LEAR facility at CERN. These data have been submitted for publication.

At present the method was applied to nine targets with mass numbers between 58 and 238. A clear neutron halo effect, correlated with the neutron binding energy, B_n, was observed and is shown in Fig. 2.

The significant differences in the halo factor for nuclei with a similar Coulomb barrier (as in ^{96}Ru and ^{96}Zr or ^{144}Sm and ^{154}Sm) demonstrate that we go here beyond a rather trivial effect of the proton wave function attenuation by this barrier. Instead, the correlation of f_{halo} with the neutron separation energy, shown in Fig. 1, classifies the observed effect to the same category of phenomena (although with much smaller magnitude) as the neutron halo effects in light nuclei close to the neutron drip line.

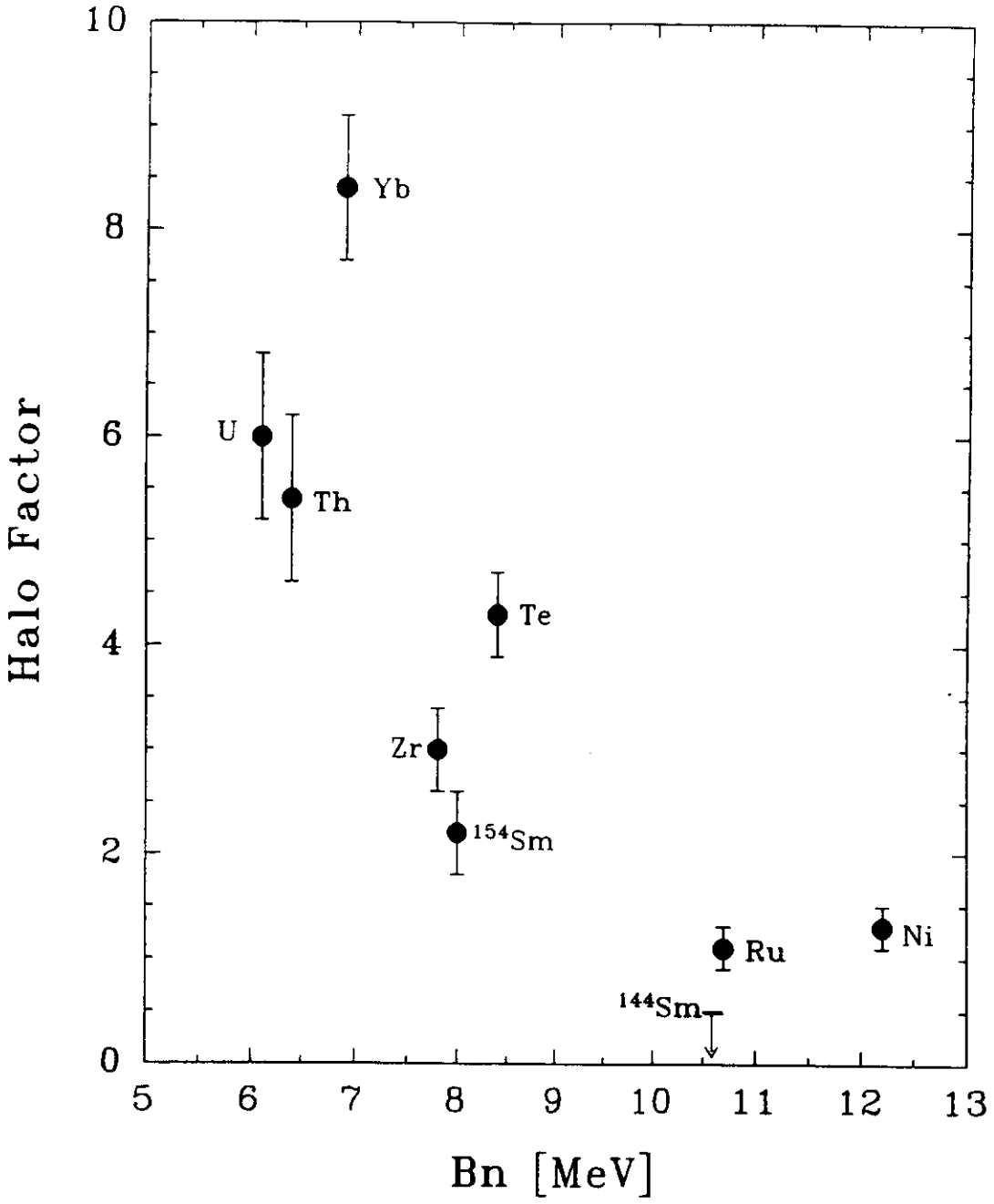

Fig. 2. *The recent data of the Warsaw - Munich collaboration (PS203), showing the neutron halo factor (defined in the text) as a function of the target neutron separation energy, B_n. The scattering of the data points indicates that the neutron halo factor depends not only on B_n, but also on some properties of the antiprotonic atom or on the nuclear sctructure.*

1.4. Calculations

In order to improve the understanding of the experimental results presented here, nuclear and atomic models have to be employed. In particular from these models one determines:

- the densities of protons $\rho(p)$ and neutrons $\rho(n)$ at large nuclear distances;
- the antiproton absorption probabilities on a proton, W_p, and on a neutron, W_n, as a function of the nuclear radius;
- the missing probability, P_{miss}, i.e. the probability that the annihilation pions do not interact with target nucleons;
- the fraction of capture events occurring on deeply bound target nucleons and leading to (A_t-1) nuclei with excitation energy above the neutron binding energy.

Calculations along these lines are presently in progress. The first results for ^{232}Th are presented in Fig. 1. Figure 3 gives the calculated neutron to proton density ratios as a function of the nuclear distance. The calculated density ratios are in qualitative agreement with the experimental data.

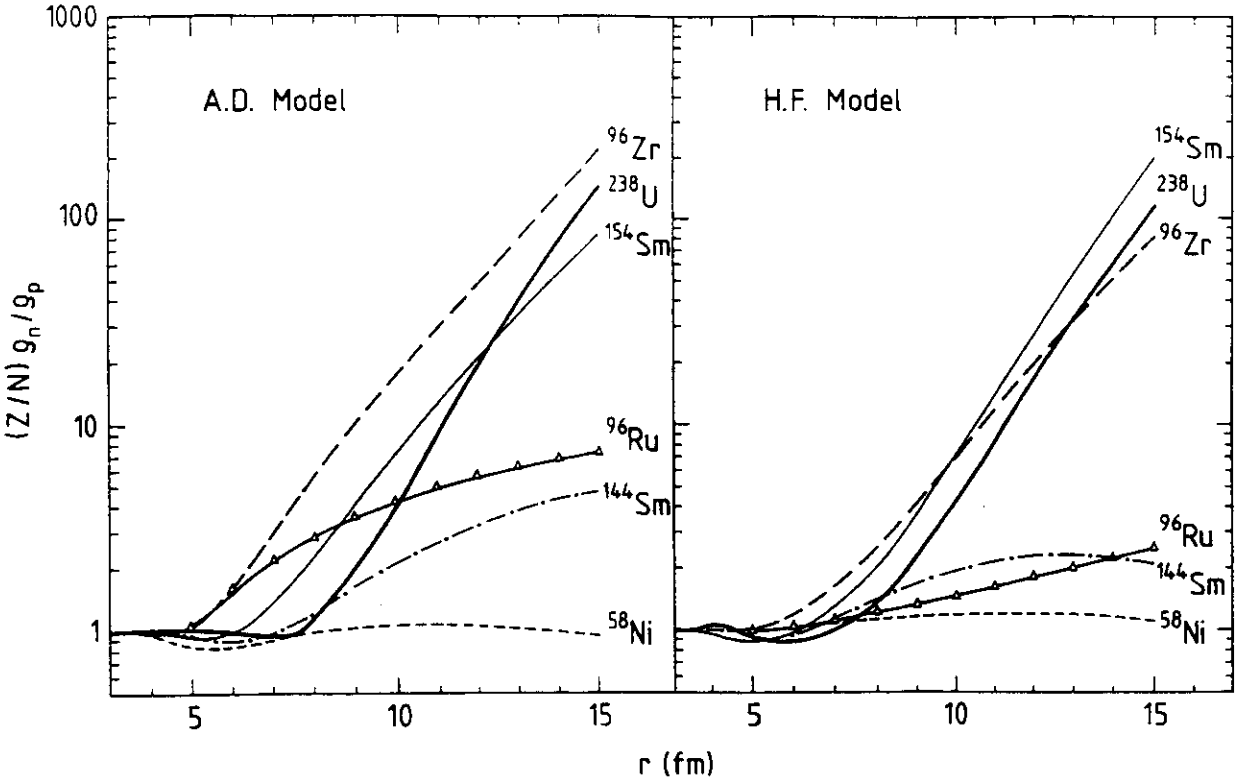

Fig. 3. *Calculated neutron to proton density ratio as a function of the nuclear distance. Left part: Asymptotic Density model. Right part: Hartree-Fock calculation (from [LUB94]).*

2. Antiproton-nucleus optical potentials

To describe nuclear interactions of antiprotons one has to use optical potentials. They are either calculated from the $N\overline{N}$ interaction models or guided by theoretical considerations. They are frequently left in a semi-phenomenological form containing free parameters. The latter involve nuclear densities folded over $N\overline{N}$ formfactors v(u) and some scattering length parameters *a*:

$$V(r) = \frac{2\pi}{\mu} a \int \rho(r-u) v(u) du$$

These optical potentials have been tested by comparison with atomic data in light nuclei coming from LEAR [ROH86], and elsewhere [ROB77]. The simplest form of V(r) contains two strength parameters Re(*a*) and Im(*a*) for the real and absorptive parts and two corresponding range parameters Re(r0), Im(r0) involved in v(u). The level shifts and widths in the oxygen region have been used to determine the best *a* value [BAT81a, BAT81b, BAT87, BAT89]. This fit has been obtained with plausible values of the range parameters and indicates a rather weak isospin dependence of *a*.

Optical potentials calculated from the $N\overline{N}$ interaction models are in general of more complicated forms, involving gradients and terms non-linear in the density. Those differ in the approach and approximations [GRE82, WON84, ADA85, DUM86, SPA87]. In particular the asymptotic form at large radii that determines the atomic levels depends on the treatment of the uncertain off-shell behaviour in the $N\overline{N}$ system. Although most potentials yield attraction at very large distances, already at 10 % density various calculated potentials differ sizeably and become less certain. This reflects complicated interplay of nuclear medium effects and strong attraction and absorption in the $N\overline{N}$ system. The shape of potentials at these and larger densities is of interest in the context of the nuclear Coulomb assisted quasi-bound states of antiprotons [BAT91, WYC93], undetected so far by direct $(\overline{p},p)$ experiments [GAR85]. The existing experimental atomic data are reproduced by this theoretical input with typically 20 % discrepancy, although some isotope effects may be reproduced better than that [GRE87].

None of these potentials explains large nuclear LS coupling [KRE88a]. This coupling reflects interplay of the long range pion exchange forces with the annihilation mechanisms. The discrepancy probably is caused by uncertainties of the annihilation in the channel of the vacuum quantum numbers $^{13}P_0$ [WYC90].

C. PROPOSED EXPERIMENT: MEASUREMENTS OF X-RAYS IN HEAVY ANTIPROTONIC ATOMS

1. Project motivation and objectives

The main purpose of this experiment is an extension of the nuclear surface studies and the detection of the neutron halo in heavy nuclei .The previous experiment [PS203] was set to identify nuclei produced in the nuclear capture of antiprotons from atomic states. A clear evidence of a neutron halo was obtained in a series of nuclei (see Sec. B1). It is of interest to learn about the properties of atomic cascade and energy levels of antiprotonic atoms of the same nuclei.

So far the interpretation of the neutron halo measurements has been done in terms of antiproton-nucleus optical potentials. The latter allow to estimate the states of nuclear capture and the wave function of the antiproton in the nuclear region. Then one can obtain information on the relative neutron/proton density distribution and test it in comparison with nuclear models.

There is no stringent test of optical potentials in heavy nuclei, however, neither from phenomenological nor from theoretical point of view. The existing data consist of: E2 mixing measurements [WYC90] which may fix only an area in Re(a), Im(a) length space, the spin-orbit splitting measurement in Yb [KRE88a] and rather old, pre-LEAR, measurements of level widths and shifts [ROB77] in some medium-heavy nuclei. There is no overlap of these measurements with the targets used to determine the neutron halo.

The motivation of this experiment is therefore to:

- test the antiproton optical potential in heavy nuclei,
- fix the atomic cascade and the states of nuclear capture in those nuclei where the neutron halo can be detected by radiochemical methods. As a by-product of this measurement we may
- investigate the antiproton-nucleus LS coupling in some nuclei, and improve our understanding of its isospin structure.

2. Expectations from theory

To test the future analysis we present in Table 1 and Figs. 4,5 the sensitivity of some measured quantities to the optical potential parameters. These quantities are: ε_{low} - lower level shift, Γ_{low} - lower level width, Γ_{up} - upper level width measured in the X-ray experiments. The other numbers are: {A-1} - the ratio of antiproton capture on a single nucleon to the total capture and {n/p} - the ratio of capture on neutrons relative to protons measured by the radiochemical methods in the PS203 experiment. The last entry is a signature for the neutron halo. All numbers are calculated for ^{232}Th with the same nuclear density calculated with a

Table 1.

Optical potential	B0	GW	B1	B2	
ε_{low}	78	302	21	-229	eV
Γ_{low}	1325	1449	1612	1920	eV
Γ_{up}	34	43	41	45	eV
{A-1}	0.15	0.20	0.14	0.09	
{n/p}	5.00	5.56	4.79	3.86	

The optical potential parameters are given by B0: a = -1.53-2.5i fm, r_0 = .8 fm [BAT81a, BAT81b]; B1: a = -1.53-2.5i fm, Re(r_0) = 1.5 fm, Im(r_0) = 1.0 fm [BAT81a, BAT81b]; GW, theoretical potential of [GRE82] and B2: a = -2.53-1.5i fm, Re(r_0) = 1.5 fm, Im(r_0) = 1.0 fm. The first three entries are close to realistic situation; the B2 entry is an arbitrary extrapolation of the best fit result of [BAT81a, BAT81b].

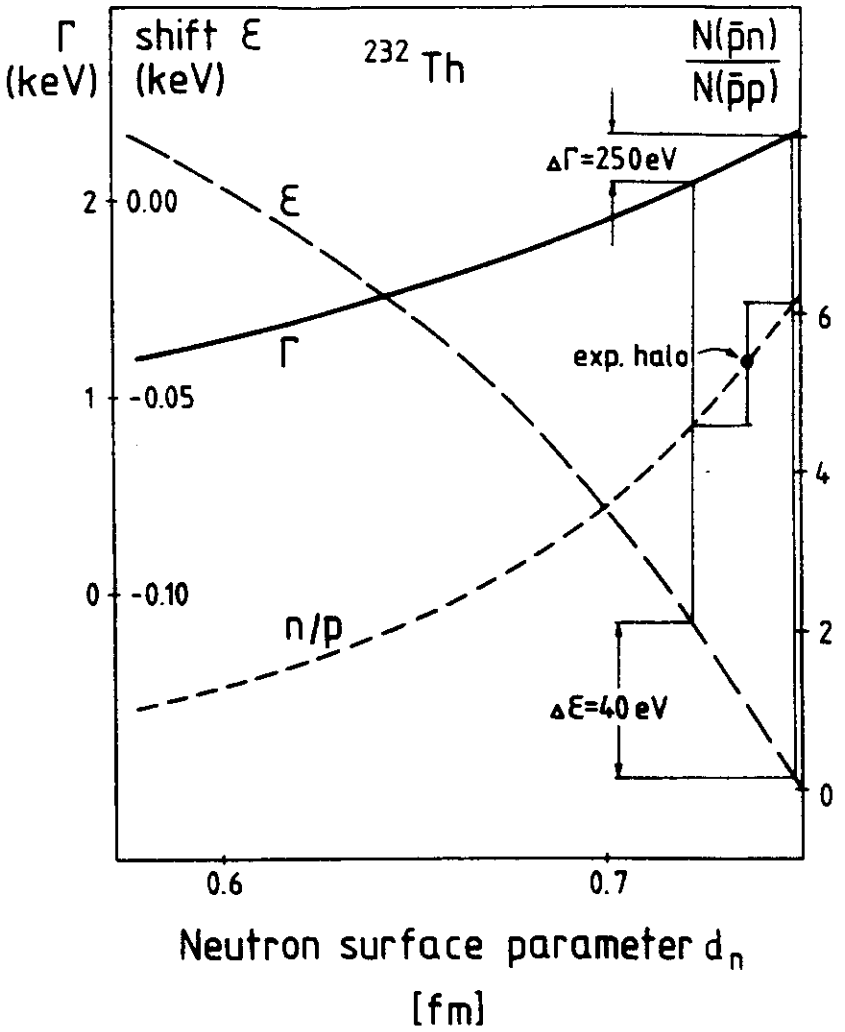

Fig. 4. Calculated n = 9, l = 8 level width and shift in ^{232}Th as a function of the neutron surface thickness parameter d_n. The calculated and experimentally determined ratio of annihilations on neutron and proton is also shown. The assumed density distribution and antiproton-nucleus potential are discussed in the text (see p. 15). Within these assumptions the indicated $\Delta\Gamma$ and $\Delta\varepsilon$ would give the same precision of the neutron surface parameter determination as the presently available neutron halo data do. As can be seen from Table 1, substantially larger errors on Γ and especially on ε would still clearly restrain the acceptable potentials.

These results indicate a larger effect of the optical potential on: ε_{low}, Γ_{low} and {A-1} ratio than on the {n/p} ratio. This is fortunate for the experiment proposed. The limitations obtained for the optical potential parameters would allow a finer tuning of the {n/p} ratio.

The neutron density distribution at large radii is not known, however. The PS203 experiment tests, essentially, the {n/p} ratio while the X-ray cascade would be more sensitive to the density itself. Correlations of the neutron halo and the level width (shift) are indicated in Fig. 4. The $n = 9$, $l = 8$ level width and shift in ^{232}Th are given as a function of the neutron density. The proton density is fixed by an experimental charge density ($c = 6.791$, $d_p = 0.571$ fm). The neutron density is the same but the surface is deformed and its thickness d_n is kept free to generate the neutron halo.

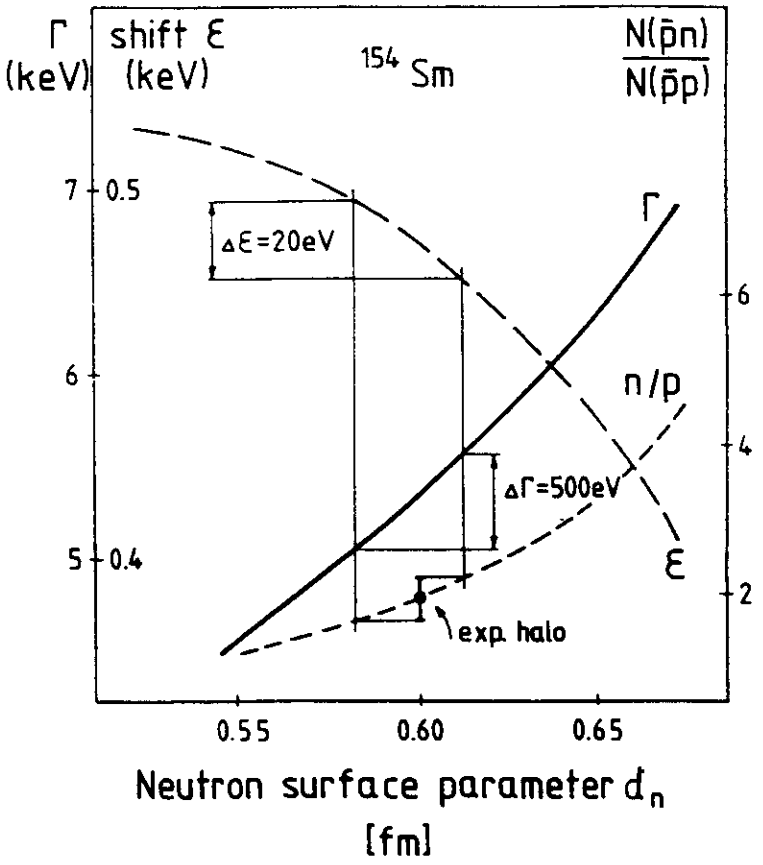

Fig. 5. The same as Fig. 4 but for the $n = 7$, $l = 6$ level in ^{154}Sm. The B0 potential is again used and $c_n = c_p = 5.938$ fm and $d_p = 0.522$ fm.

The B0 potential produces weakly repulsive level shifts. This is a result of cancellations. The effect of the attractive real part is cancelled against the repulsion due to the absorptive part. This delicate balance is affected by the relative Im(a_n)/Im(a_p) and Re(a_n)/Re(a_p). The former ratio of 0.63 has been taken from the absorption data in carbon [BUG73], the latter ratio is taken to be 1 as this number follows from theoretical models. This assumption enhances the attractive effects and yields attractive level shifts. In light nuclei these shifts are known to be repulsive but the measurements done on one heavy target - ^{174}Yb [ROB77, KRE88a] yield an attractive shift. The latter is probably due to the E2 mixing [GRE88] but to clarify the

could be analysed together with the existing data on the dynamic E2 mixing [WYC93] which indicate repulsive shifts for levels deeper than those discussed here (to be seen by the direct line shape measurements).

The {n/p} halo is more sensitive to the surface parameter - d - than the level width but the extended neutron density surface is seen to make a 50 % contribution to the latter and even more to the upper widths [WYC93]. Thus the measurement of two level widths done jointly with {A-1} and {n/p} ratio (PS203) would be rather restrictive on the neutron density distribution.

Table 2
Atomic transitions to be observed

Element	n → n'		Transition energy, keV	Absorptive width, eV	Strong int. shift, eV	Relative yield, %
^{58}Ni	7	6	142.9	12		
	6	5	236.77 237.67	1500	130	16
^{96}Ru	7	6	353	3030	230	12
^{96}Zr	8	7	190.29 190.83	14		
	7	6	293.37 294.70	1200	70	31
^{144}Sm	9	8	314.87 316.31	114		
	8	7	459.36 462.61	5170	500	9
^{176}Yb	10	9	287.29 288.46	37		
	9	8	401.83 404.18	1200	250	30
^{232}Th	11	10	351.96 353.67	42		
	10	9	475.91 479.12	1500	470	40
^{238}U	11	10	367.85 369.72	50		
	10	9	497.40 500.89	1700	490	40

Expected antiprotonic atomic cascade transitions. Only circular levels are considered and the two main fine structure transitions $j = l + 1/2 \rightarrow j' = l + 1/2 - 1$ *and* $j = l - 1/2 \rightarrow j' = l - 1/2 - 1$ *are presented. The X-ray energies include electromagnetic values only. Optical model estimates are given for the absorptive level widths, level shifts and relative yields of the last*

The third motivation of X-ray measurements is a confirmation of the anomalously large antiproton-nuclear LS coupling [KRE88a] detected in ^{174}Yb and so far not explained by the existing $N\overline{N}$ interaction models. Possibly this large effect is related to the annihilation properties in the $^{13}P_0$ state [WYC90]. As indicated in Table 2 we have a good chance to see the LS splitting in ^{176}Yb, Th and U targets.

It has to be stressed that these results would be obtained in addition and simultaneously with the main measurement.

COMMENTS to Table 2.

Zr

The X-rays in ^{nat}Zr were observed in the pre-LEAR era [ROB77]. For the lower level a repulsive shift of 450(100) eV and widths of 700(210) eV (lower level) and 6.4(+1.7/-1.33) eV (upper level) have been obtained. Our intention is to repeat this measurement with a higher precision and with isotopically separated target. In our list the ^{96}Zr nucleus is the heaviest spherical nucleus which allows precise atomic measurement. It will facilitate theoretical analysis of strong interactions.

Sm

The cascade is less favourable in this case and the chance to reach the low broad level of n = 7 is small. One advantage of this measurement, if successful, would be an indirect information on nuclear quasi-bound state of antiprotons. Possibilities of such states have been discussed for a long time but the direct ($\overline{p}$,p) experiments [GAR85] have not found clear signals because of a high background.

An indirect information may be obtained from atomic studies [BAT91] since a state of this kind sizeably affects an adjacent deeply bound atomic state. Till now, indications of deeply bound atomic states of about 10 keV widths were detected only indirectly via the E2 effect in ^{130}Te and ^{150}Sm [WYC93]. These E2 mixing measurements can be applied only in special regions of atomic widths and shifts.

In any case the measurement would provide the upper widths which could be compared to the upper widths obtained for ^{152}Sm [WYC93]. The fine structure has been resolved in the latter case and an evidence of a strong antiproton-nucleus spin-orbit force followed [WYC93].

Yb

Previous measurements at LEAR were done for ^{174}Yb. For the first time the fine structure was resolved, in consequence very strong spin-orbit nuclear interaction has been established [KRE88a]. The strength of this interaction is not well understood in terms of potential $N\overline{N}$ interactions [WYC90]. A measurement for ^{176}Yb would confirm the previous finding, establish the isotope effect and possibly give some information on the dependence of the spin - orbit force on nuclear deformation.

Th, U

These targets offer high chances to reach "the lower" atomic states. However, X-rays of 500 keV have to be detected. Such energies lie beyond the region of antiprotonic X-rays observed so far.

D. EXPERIMENTAL CONSIDERATIONS

1. Overview

The determination of the line width with the precision of $\Delta\Gamma \cong 70$ eV and of $\Delta\mathcal{E} \cong 40$ eV for gamma-ray energies in the range of 200 - 500 keV is presently the state of the art using modern HP Germanium detectors with well stabilised electronics. As it was indicated in the caption to Fig. 4 these values are sufficient to be compared with the neutron halo results and to restrain substantially the optical model parameters.

The experiment will be performed using three HP Germanium detectors, two of which are already available and the third one will be purchased if this proposal is accepted.

An antiproton beam of 200 MeV/c with about 10^5 $\bar{p}$ps, delivered in 1 - 2 h long spills is anticipated for this experiment. As shown below, about 10^6 photo-peak counts can be collected during 5 h of running time with this $\bar{p}$ intensity. This means that it is **perfectly acceptable to run in parasitic mode**.

The first days of the experiment will be used to optimise the measuring conditions concerning background, geometry, detector resolution, etc.

Having all above considerations in mind we propose that in 1995 this experiment obtains **three weeks** of beam time in parasitic mode with $\approx 10^5$ $\bar{p}$ps of 200 MeV/c. The antiproton momentum of 100 MeV/c or 300 MeV/c is also acceptable. Below some aspects of the proposed experiment are presented in more details.

2. Layout of the experiment

At present we suppose that the experiment will be placed on the beam line C1. Fig. 6 presents the position of the main parts of the experimental setup and Fig. 7 the schematic view of the target - counters ensemble.

The S0 counter is used as an active diaphragm, working in anticoincidence with S1 antiproton counter. Both counters are made of NE212 scintillator 2-3 mm thick. The beam degrador made of mylar will degrade the antiproton energy from 22 MeV to about 7 MeV.

Charged π produced in the target will be rejected by S2, S3 and S4 counters, inhibiting the Ge detectors. These counters will be also made from 2-3 mm thick plastic scintillator, NE212.

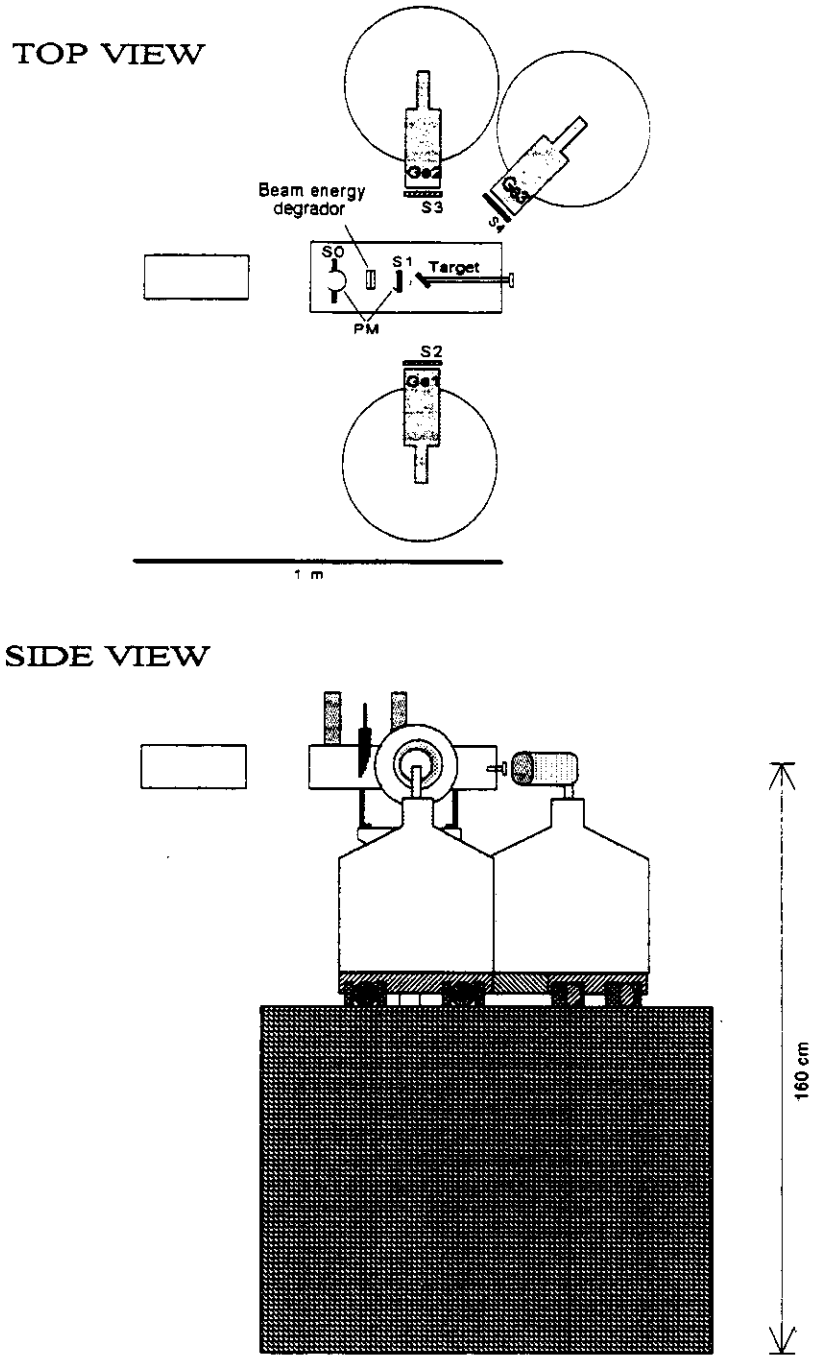

Fig. 6. The general view of the main parts of the experimental setup.

The coincidence between S1 and Ge counters together with the event by event data acquisition will allow to measure simultaneously the antiprotonic X-ray spectra and the gamma lines from calibration sources. If necessary, this way of operation can facilitate the gain shift corrections during the off-line data analysis.

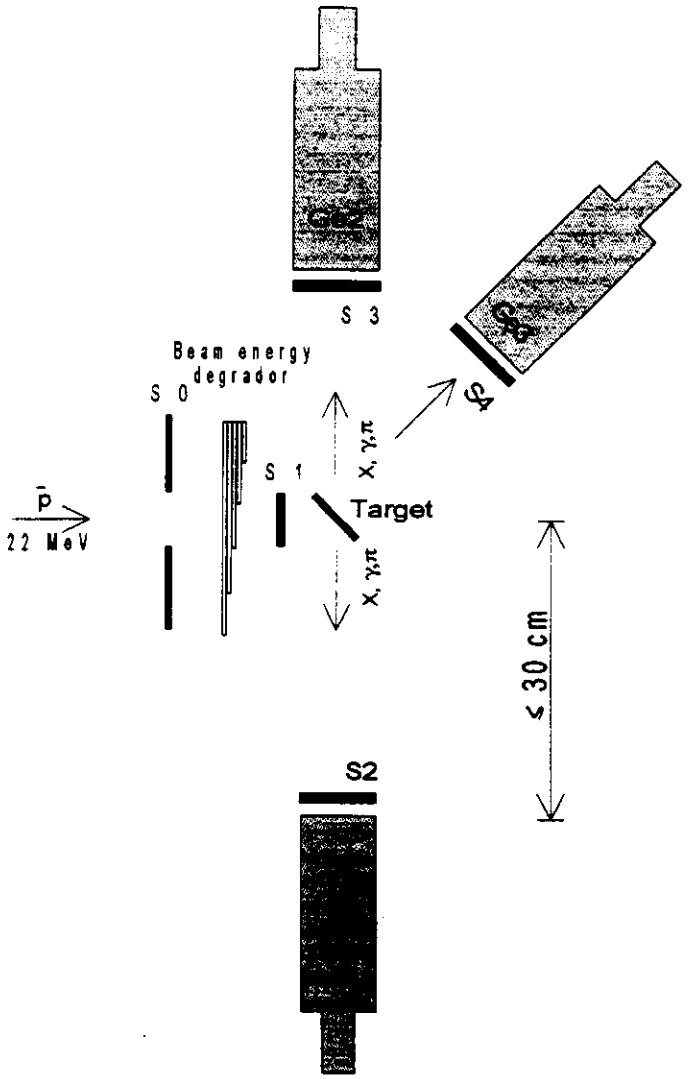

Fig. 7. The schematic view of the target - counter ensemble.

3. Ge detectors

Below we present some characteristics of already available detectors. Ge1 is a 93.7 cm^3 19.4 % relative efficiency n-type true coaxial detector made by ORTEC. Ge2 is a 124.4 cm^3 30 % relative efficiency p-type coaxial detector made by CANBERRA. Ge3 is a n-type planar Ge detector of 6.4 cm^3 made by ORTEC. Most probably Ge2 will be replaced by another detector of larger volume than Ge3.

Fig. 8 present the absolute photo-peak efficiencies of these detectors. In Fig. 9 and Fig. 10 are shown photo-peak resolutions (FWHM) for Ge1, Ge2 as a function of the counting rate and in Fig. 11 as a function of the gamma ray energy for all detectors. ORTEC 672 model amplifier was used for Ge1, Ge3 and CANBERRA 2020 model amplifier was used for Ge2. The pulse time shaping was 6 μs.

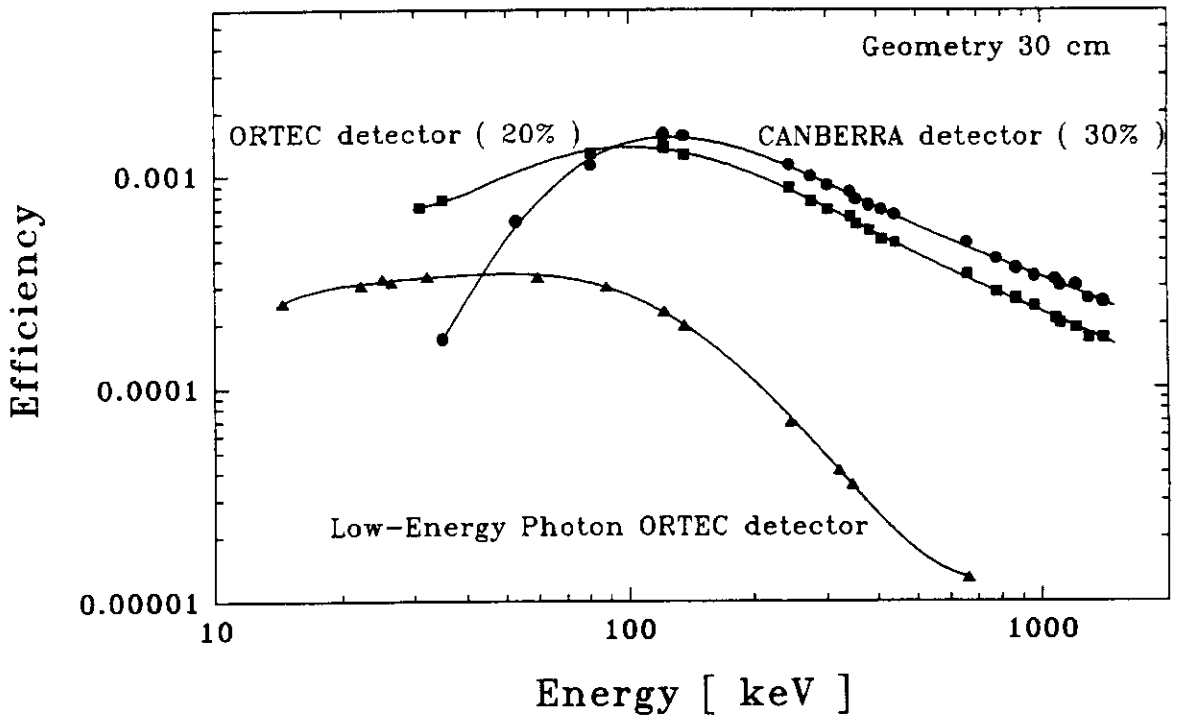

Fig. 8. The absolute photo-peak efficiencies of available Ge detectors.

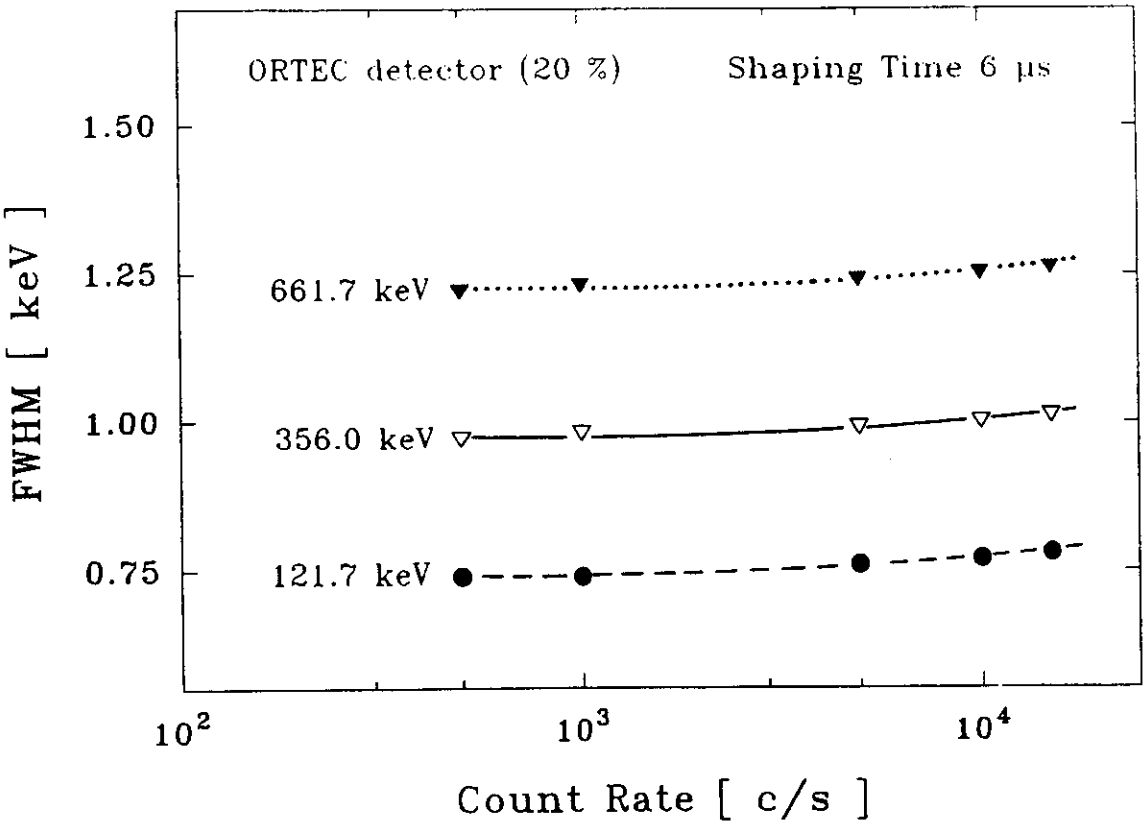

Fig. 9. Photo-peak resolution (FWHM) as a function of the counting rate for the ORTEC

The gain and zero stability of Ge detectors is crucial for the success of the proposed experiment. As it was mentioned in Sect. 4 some off-line correction of the gain shifts will be possible. The presently observed gain and zero stability of our detectors - electronics is illustrated in Fig. 12 for gamma-X ORTEC detector. These data are obtained with standard 8k Tennelec\Nucleus PCA II pulse-height analyser connected to IBM PC AT computers.

The purchase of 8k ADC and of the gain - zero (two-point) stabiliser is planed for the proposed experiment.

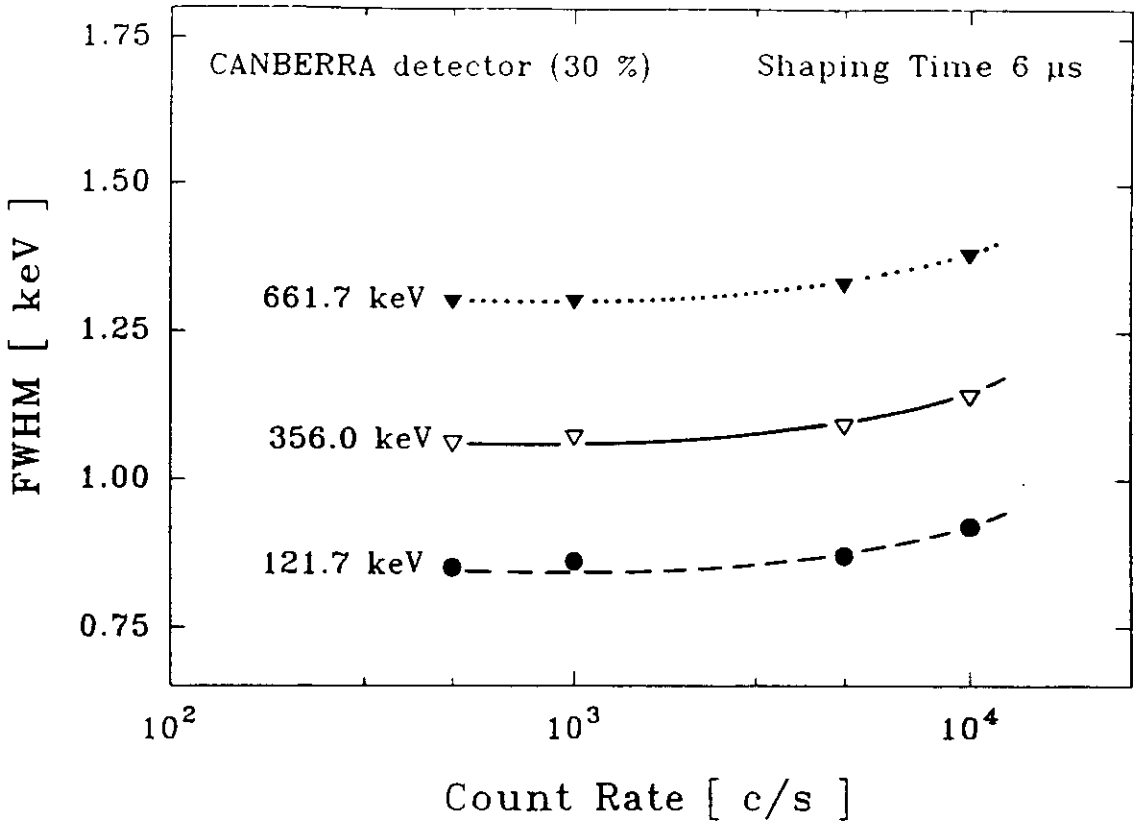

Fig. 10. Photo-peak resolution (FWHM) as a function of the counting rate for the CANBERRA detector.

4. Data acquisition

The data acquisition system will use the Camac ADC and TDC (Ge - S1). Data will be readout and temporary stored in list-mode by front-end processor (STARBURST). From the front-end processor data will be transferred in DMA (Direct Memory Access) mode to the back-end computer (DEC ALPHA) and written on EXABYTE tape. The back-end processor will also build and display histograms from the accumulated data. The response time of the front-end processor is very small: around 10 μs between hardware trigger and the start of the read-out. The system described was successfully used during PS202 and PS205 experiments

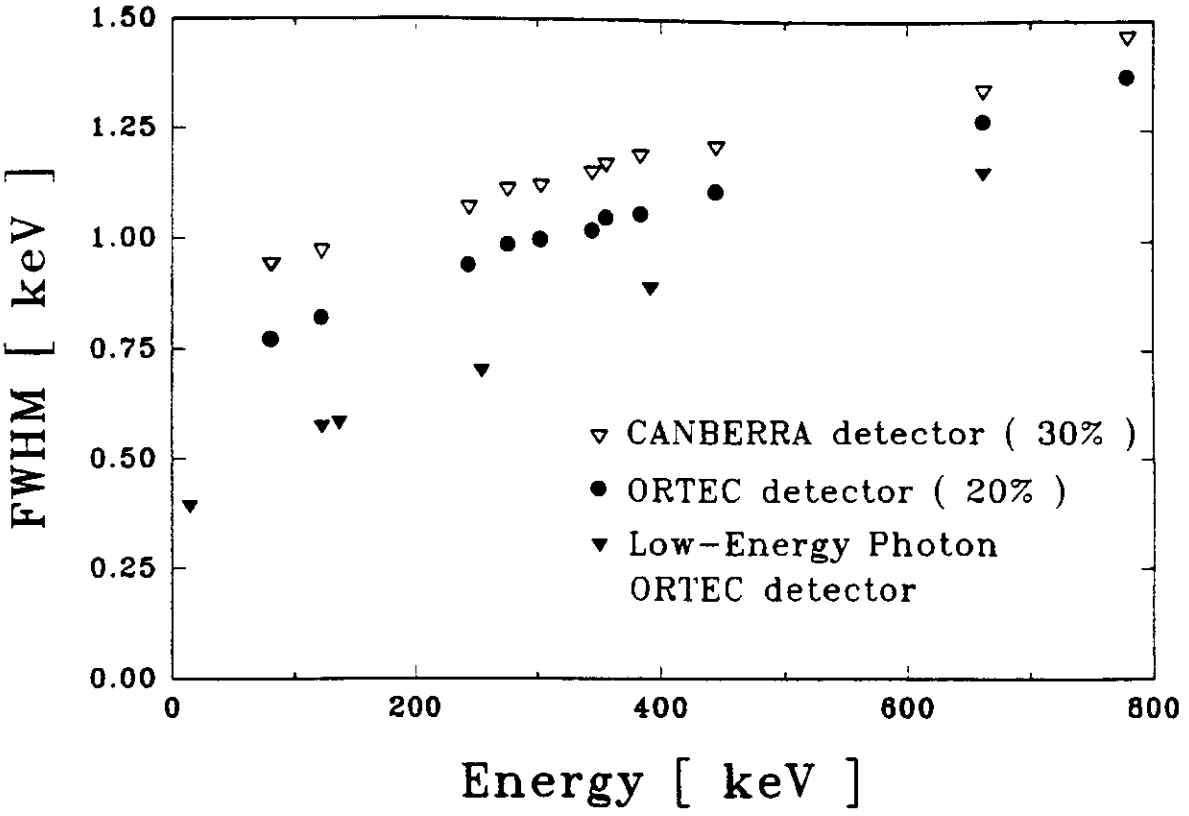

Fig. 11. Photo-peak resolution (FWHM) as a function of the gamma-ray energy for three available detectors.

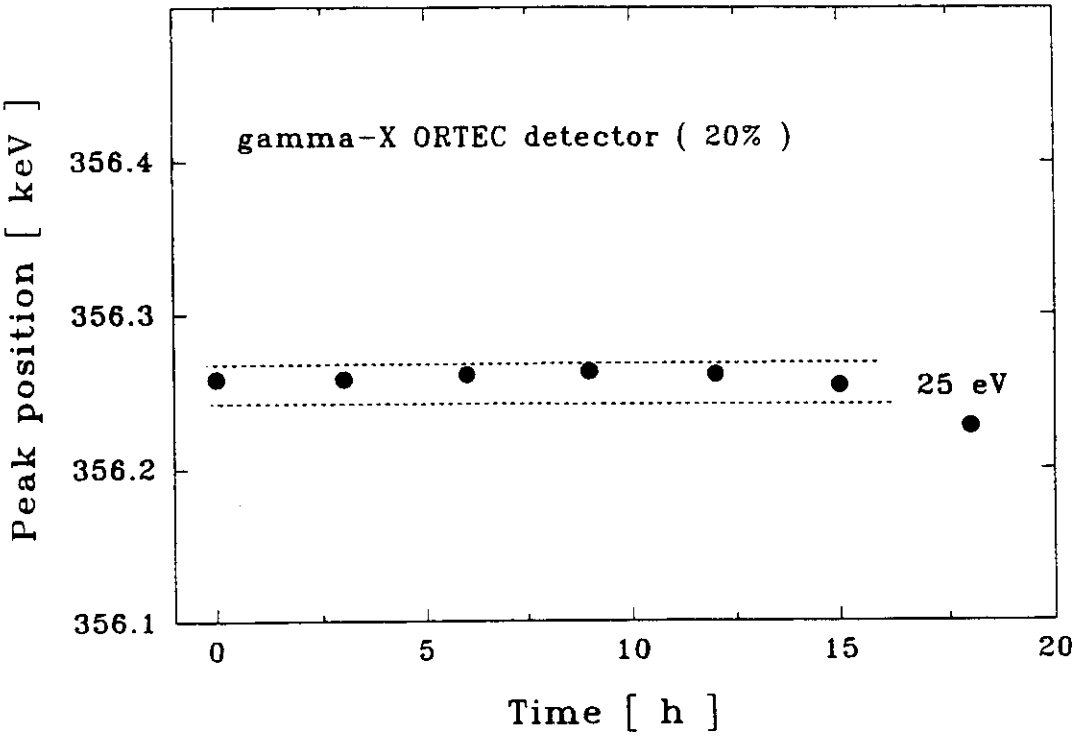

Fig. 12. The test of the gain and zero stability for the ORTEC detector assembly. The channel position of the 356 keV photo-peak is plotted versus the measurement time. Temperature was maintained within ± 1°C. No gain stabiliser was used.

5. Targets

Targets will be placed in thin plexiglas frames. In case of natural targets their dimension will be about 3x3 cm^2 with a thickness of about 100 mg/cm^2. Isotopically separated targets, in most cases already available, will be smaller ($\approx$ 1.5x1.5 cm^2) and thinner (between 30 and 50 mg/cm^2).

In order to determine the absolute number of antiproton annihilations in targets of thickness smaller than the antiproton range straggling, the method described in Ref. [LUB94] will be used. In short the method consists of off-line ^{24}Na activity determination in Al foils (thicker than $\bar{p}$ range straggling) with and without target (to be used for X-ray measurements) between them.

6. Estimation of counting rates

The main loading of Ge detectors will not be due to the gamma (X) rays but rather to pions after antiproton annihilation in the target and outside of it and to the energetic charged particles from highly excited target nuclei.

In order to estimate the Ge detector counting rates and loading we make the following simplifing assumptions:

$\pi^{\pm}$	energy	200 MeV	
π^0		neglected	
$\pi^{\pm}$	multiplicity	2.5	(see PS203)
p	energy	50 MeV	
p	multiplicity	1.0	(see PS203)
Z > 1	particles	neglected	(from PS203 d multiplicity is 0.1 and lower for higher Z particles)
X-ray	energy	200 keV	
X-ray	multiplicity	10	
$\bar{p}$	beam intensity	10^5/sec	(entirely stopped in the target)

The following table compares the estimate for gamma-X ORTEC and Low-Energy Photon ORTEC detectors previously described:

	Gamma-X ORTEC detector (Distance 30 cm)	Low-Energy Photon ORTEC detector (Distance 10 cm)
Detector surface	1892 mm^2	491 mm^2
Detector thickness	49 mm	13 mm
Solid angle (% 4Π)	0.16	0.34
γ-ray efficiency (200 keV)	1.0	0.8
π efficiency	1	1
p efficiency	1	1
π energy loss (E_π = 200 MeV)	37 MeV	10 MeV
p energy loss (E_p = 50 MeV)	50 MeV	50 MeV
counting rates (10^5 $\bar{p}$ stopped in the target)		
X-rays	1860/sec	2860/sec
π	400/sec	850/sec
p	160/sec	340/sec
Energy deposition rate	23 000 MeV/sec	25 000 MeV/sec
Preamplifier rate limit (from producer)	140 000 MeV/sec	≈ 30 000 MeV/sec
γ Peak /Total ratio (200 keV)	0.55	0.32
Single photopeak counting rate	102/sec	92/sec

About 10^6 counts in a photopeak will be collected during 5 h of measuring time with 10^5 $\bar{p}$ps. Pions and charged particles will overload the X and γ-X detectors. For both detectors the recovery time will be comparable so the γ-X detector will perform better due to lower rate. However energy resolution is better for the X detector by about 25 %. Plastic scintilators in front of detectors will prevent triggering data acquisition during overload (anticoincidence).

E. SUMMARY AND CONCLUSIONS

We are deeply convinced that the experiments proposed here will substantially improve our knowledge of the nuclear periphery in heavy nuclei and will clearly delimit the range of parameters defining the antiproton-nucleus optical potential. Our previous experience over many years in in-beam gamma-ray studies and exotic atom investigations as well as the direct participation in this project of a theory group with a world wide recognised expertise in antiproton-nucleus physics will put this study on a firm experimental and theoretical ground.

We are evidently aware of the pressure existing on the LEAR beam time during the next two years. On the other hand the experiment we propose could be the last chance for the study of antiprotonic X-rays in heavy nuclei perhaps forever.

References

[ADA85] S. Adachi, H.V. von Geramb, Acta Phys. Aust. **XXXVII** (1985) 627.

[ASL70] K. Aslam, J.R. Rook, Nucl. Phys. **B20** (1970) 397.

[BAT81a] C.J. Batty, Nucl. Phys. **A372** (1981) 418.

[BAT81b] C.J. Batty, Nucl. Phys. **A372** (1981) 433.

[BAT87] C.J. Batty, Phys. Lett. **B189** (1987) 393.

[BAT89] C.J. Batty, E. Friedman, H.J. Gils, H. Rebel, Adv. Nucl. Phys. **19** (1989) 1.

[BAT91] C.J. Batty, E. Friedmann, A. Gal, G. Kalberman, Nucl. Phys. **A535** (1991) 5.

[BUG73] W.M. Bugg, G.T. Condo, E.L. Hart, H.O. Cohn, R.D. McCulloch, Phys. Rev. Lett. **31** (1973) 475.

[BUR67] E.H.S. Burhop, Nucl. Phys. **B1** (1967) 438.

[BUR72] E.H.S. Burhop, Nucl. Phys. **B44** (1972) 445.

[DAN87] H. Daniel, F.J. Hartmann, W. Kanert, H. Plendl, T. von Egidy, J.J. Reidy, H. Koch, A. Kreissl, H. Poth, D. Rohmann, Z. Phys **A326** (1987)523.

[DAV67] D.H. Davis, S.P. Lovell, M. Csejthey-Barth, J. Sacton, G. Schorochoff, M. O'Reilly, Nucl. Phys. **B1** (1967) 434.

[DUM86] O. Dumbrajs, H. Heiselberg, A.S. Jensen, A. Miranda, G.C. Oades, J.M. Richard, Nucl. Phys. **A457** (1986) 491.

[GAR85] D. Garreta, P. Birien, G. Bruge, A. Chaumeaux, D.M. Drake, S. Janouin, D. Legrand, M.C. Lemaire, B. Mayer, J. Pain, J.C. Peng, M. Berrada, J.P. Bocquet, E. Monnand, J. Mougey, P. Perrin, E. Aslanides, O. Bing, J. Lichtenstadt A.I. Yavin, Phys. Lett. **150B** (1985) 95.

[GER74] W.J. Gerace, M.M. Sternheim, J.F. Walker, Phys. Rev. Lett. 33 (1974) 508.

[GRE82] A.M. Green, S. Wycech, Nucl. Phys. **A377** (1982) 441.

[GRE87] A.M. Green, S. Wycech, Nucl. Phys. **A467** (1987) 744.

[GRE88] A.M. Green, G.Q. Liu, S. Wycech, Nucl.Phys. **A483** (1988) 419.

[HAN87] P. G. Hansen, B. Jonson, Europhys. Lett. **4** (1987) 409.

[HAN91] P. G. Hansen, Nucl. Phys. News **1** (1991) 21.

[JAC74] D.F. Jackson, Rep. Prog. Phys. **37** (1974) 55.

[JAS93] J. Jastrzębski, H. Daniel, T.von Egidy, A. Grabowska, Y.S. Kim, W. Kurcewicz, P. Lubiński, G. Riepe, W. Schmid, A. Stolarz, S. Wycech, Nucl. Phys. **A558** (1993) 405c.

[JOH54] M.H. Johnson, E. Teller, Phys. Rev. **93** (1954) 357.

[JON58] P.B. Jones, Phil. Mag. **3** (1958) 33.

[KAN86] W. Kanert, F.J. Hartmann, H. Daniel, E. Moser, G. Schmidt, T. von Egidy, J.J. Reidy, M. Nicholas, M. Leon, H. Poth, G. Büche, A.D. Hancock, H. Koch, Th. Köhler, A. Kreissl, U. Raich, D. Rohmann, M. Chardalas, S. Dedoussis, M. Suffert, A. Nilsson, Phys. Rev. Lett. **56** (1986) 2368.

[KRA91] A. Krasznahorkay, J. Bacelar, J.A. Bordewijk, S. Brandenburg, A. Buda, G. van 't Hof, M.A. Hofstee, S. Kato, T.D. Poelhekken, S.Y. van der Werf, A. van der Woude, M.N. Harakeh, N. Kalantar-Nayestanaki, Phys. Rev. Lett. **66** (1991) 1287.

[KRE88a] A. Kreissl, A.D. Hancock, Th. Köhler, H. Poth, U. Raich, D. Rohmann, A. Wolf, L. Tauscher, A. Nilsson, M. Suffert, M. Chardalas, S. Dedoussis, H. Daniel, T. von Egidy, F. J. Hartmann, W. Kanert, H. Plendl, G. Schmidt, J.J. Reidy, Z. Phys. **A329** (1988) 235.

[KRE88b] A. Kreissl, A.D. Hancock, H. Koch, Th. Köhler, H. Poth, U. Raich, D. Rohmann, A. Wolf, L. Tauscher, A. Nilsson, M. Suffert, M. Chardalas, S. Dedoussis, H. Daniel, T. von Egidy, F.J. Hartmann, W. Kanert, H. Plendl, G. Schmidt, J.J. Reidy, Z. Phys. **C37** (1988) 557.

[LUB94] P. Lubiński, J. Jastrzębski, A. Grochulska, A. Stolarz, A. Trzcińska, W. Kurcewicz, F.J. Hartmann, W. Schmid, T. von Egidy, J. Skalski, R. Smolańczuk, S. Wycech, D. Hilscher, D. Polster, H. Rossner, to be publ.

[NEG70] J.W. Negele, Phys. Rev. **C1** (1970) 1260.

[NOL69] J.A. Nolen Jr., J.P. Schiffer, Annu. Rev. Nucl. Sci. **19** (1969) 471.

[POT85] H. Poth, P. Blüm, G. Büche, S. Carius, S. Charalambus, M. Chardalas, S. Dedoissis, C. Findeisen, A.D. Hancock, J. Hauth, H. Koch, T. Köhler, A. Kreissl, A. Nilsson, U. Raich, D. Rohmann, M. Suffert, L. Tauscher, A. Wolf, T. von Egidy, F. Hartmann, W. Kanert, G. Schmidt, J.J. Reidy, Proceedings of the THIRD LEAR WORKSHOP, Tignes-Savoie-France, January 19-26, 1985.

[ROB77] P. Roberson, T. King, R. Kunselman, J. Miller, R.J. Powers, P.D. Barnes, R.A. Eisenstein, R.B. Sutton, W.C. Lam, C.R. Cox, M. Eckhause, R.J. Kane, A.M. Rushton, W.F. Vulcan, R.E. Weslh, Phys. Rev. **C16** (1977) 1945.

[ROH86] D. Rohmann, H. Barth, A. D. Hancock, H. Koch, Th. Köhler, A. Kreissl, H. Poth, U. Raich, A. Wolf, L. Tauscher, M. Suffert, , M. Chardalas, S. Dedoissis, A. Nilsson, W. Kanert, T. von Egidy, F. Hartmann, G. Schmidt, J.J. Reidy, Z. Phys. **A321** (1986) 261.

[SPA87] D.A. Sparrow, Phys. Rev. **C35** (1987) 1410.

[TAN92] I. Tanihata, D. Hirata, T. Kobayashi, S. Shimoura, K. Sugimoto, H. Toki, Phys. Lett **B289** (1992) 261.

[WIL59] D.H. Wilkinson, Phil. Mag. **4** (1959) 215.

[WON84] C.Y. Wong, A.K. Kerman, G.R. Satchler, A.D. Mackellar, Phys. Rev **C29** (1984) 574.

[WYC71] S. Wycech, Nucl. Phys. **B28** (1971) 541.

[WYC90] S. Wycech, H. Poth, R.J. Rook, Z. Phys. **A335** (1990) 355.

[WYC93] S. Wycech, F.J. Hartmann, H. Daniel, W. Kanert, H.S. Plendl, T.von Egidy, J.J. Reidy, M. Nicholas, L.A. Redmond, H. Koch, A. Kreissl, H. Poth, D. Rohmann, Nucl. Phys. **A561** (1993) 607.